Supplementary materials

for

Nanopore-based enzyme-assisted biomarker detection method for chronic obstructive pulmonary disease

Qianyuan Ren,[1] Yakun Yi,[1,*] Shihong Li[2,*]

Affiliations:

[1]Beijing National Laboratory for Molecular Sciences, Key Laboratory of Analytical Chemistry for Living Biosystems, Institute of Chemistry, Chinese Academy of Sciences, Beijing 100190, China.

[2]Department of Respiratory and Critical Care Medicine, Beijing Institute of Respiratory Medicine and Beijing Chao-Yang Hospital, Capital Medical University, Beijing 100020, China.

[*]To whom correspondence should be addressed. Email: yiyakun@iccas.ac.cn or lshltz1@163.com

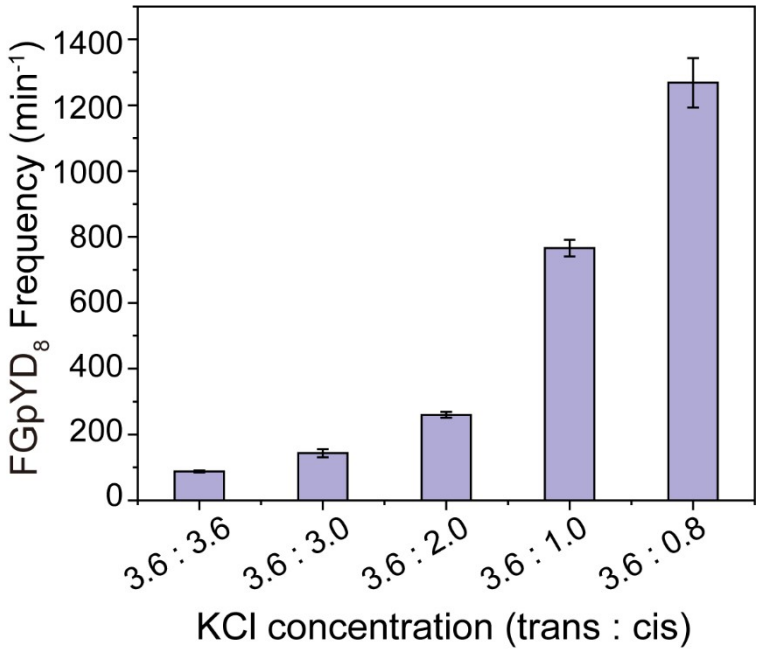

Supplementary Figure 1. Optimization of salt concentration for nanopore detection. Our previous study showed that peptides $FGXD_8$ could be discriminated when translocated through αHL nanopore in the buffer of 3.6 M KCl, 10.0 mM citric acid, pH 5.0. However, the capture rate of the peptides is not high in symmetrical electrolyte conditions. Salt gradients across nanopores have been reported to enhance electroosmotic flow (EOF) and locally amplify the electric field at the pore entrance, thereby significantly increasing the capture efficiency of charged analytes, as demonstrated in previous nanopore studies[1-3]. Therefore, an electrolyte gradient was introduced to increase the capture frequency of the peptide probe. The results show that there is a significant increase in the event frequency when the salt concentration in cis chamber is lowered. The results show that there is a significant increase in the event frequency when the salt concentration in cis chamber is lowered. Although the condition of trans : cis =3.6 : 0.8 affords the highest capture rate, the lipid bilayer becomes fragile under this condition. Therefore, we chose the following conditions for all the nanopore measurements: 3.6 M KCl, 10.0 mM PBS, pH 5.0 in trans, 1.0 M KCl, 10.0 mM PBS, pH 5.0 in cis, with the transmembrane potential held at +200 mV.

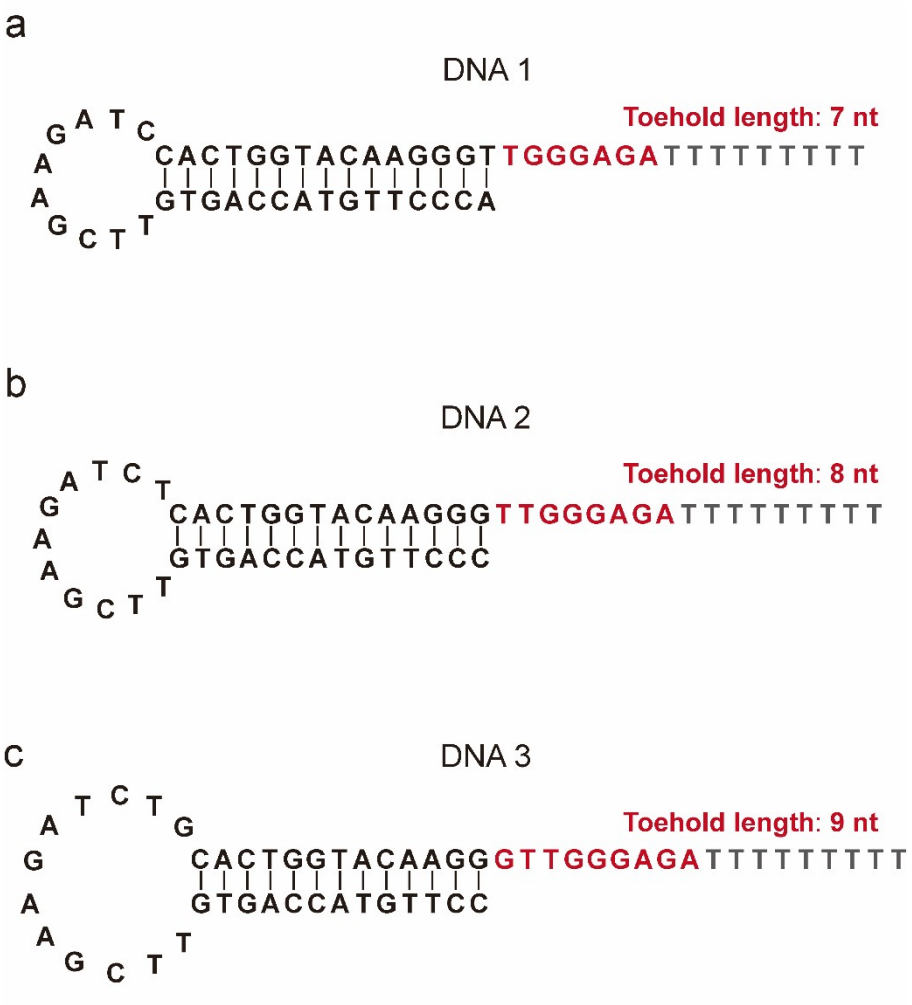

Supplementary Figure 2. Structure of different capture DNA. Hairpin structures formed by capture DNAs with different toehold lengths: **(a)** DNA 1 with a toehold length of 7 nt; **(b)** DNA 2 with a toehold length of 8 nt; **(c)** DNA 3 with a toehold length of 9 nt.

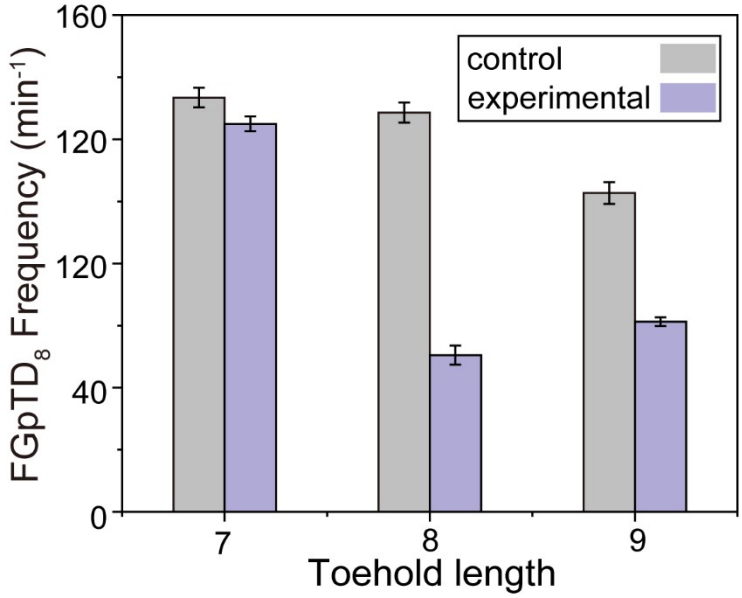

Supplementary Figure 3. Optimization of hairpin toehold length. The grey bars represent the control group, to which no target substance was added, whilst the purple bars represent the experimental group. we performed an enzyme immunoassay with 1 nM miR-150-5p (hairpin toehold tengths are 7, 8, 9, respectively). The reaction was conducted at [$FGpTD_8$] = 50.0 μM and pH 9.0. Aliquots of 2.0 μL were taken, mixed with 5.0 μL of CB[7] (5.0 mM), and added to the cis chamber for analysis. All data were acquired in the buffer of 3.6 M KCl, 10.0 mM PBS, pH 5.0 in trans, 1.0 M KCl, 10.0 mM PBS, pH 5.0 in cis, with the transmembrane potential held at +200 mV. Number of individual experiments n = 3.

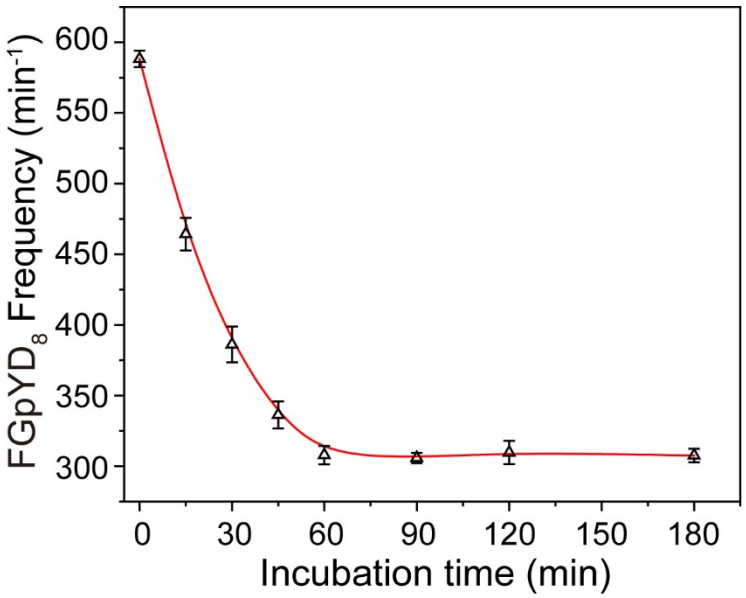

Supplementary Figure 4. Effect of reaction time on the efficiency of enzyme cleavage. To determine the saturation time for $FGpYD_8$ digestion by alkaline phosphatase, we performed an enzyme immunoassay with 100.0 ng/mL $VEGF_{165}$. The reaction was conducted at [$FGpYD_8$] = 50.0 μM and pH 9.0. Aliquots of 2.0 μL were taken, mixed with 5.0 μL of CB[7] (5.0 mM), and added to the cis chamber for analysis. All data were acquired in the buffer of 3.6 M KCl, 10.0 mM PBS, pH 5.0 in trans, 1.0 M KCl, 10.0 mM PBS, pH 5.0 in cis, with the transmembrane potential held at +200 mV. Number of individual experiments n = 3.

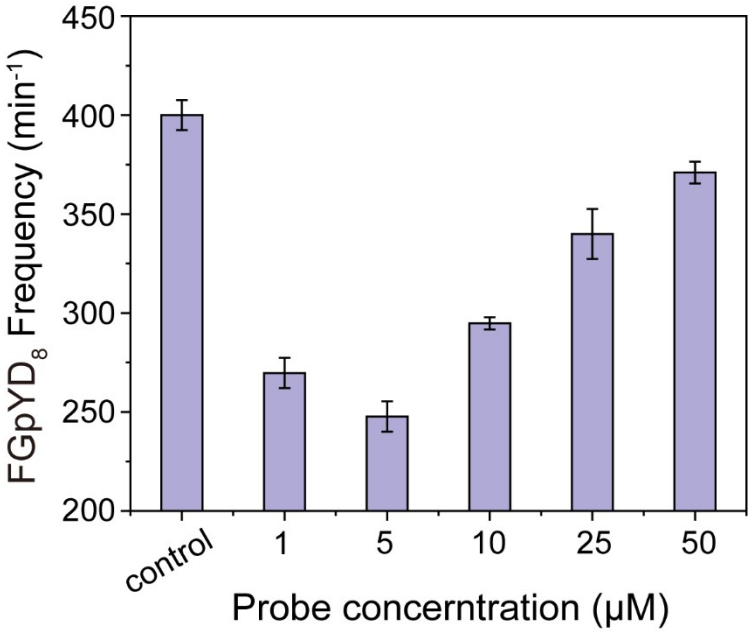

Supplementary Figure 5. Effect of the probe concentration. To determine the optimal peptide probe concentration, we performed the assay with 100.0 ng/mL $VEGF_{165}$ at different $FGpYD_8$ concentrations. The volume added to the cis chamber was adjusted for each sample, along with 5.0 μL of CB[7] (5.0 mM), to maintain a final peptide concentration of 100.0 nM in the nanopore system. The condition yielding the lowest characteristic signal frequency indicated the most efficient cleavage, leading us to select 5.0 μM $FGpYD_8$ for subsequent enzymatic reactions. All data were acquired in the buffer of 3.6 M KCl, 10.0 mM PBS, pH 5.0 in trans, 1.0 M KCl, 10.0 mM PBS, pH 5.0 in cis, with the transmembrane potential held at +200 mV. Number of individual experiments n = 3.

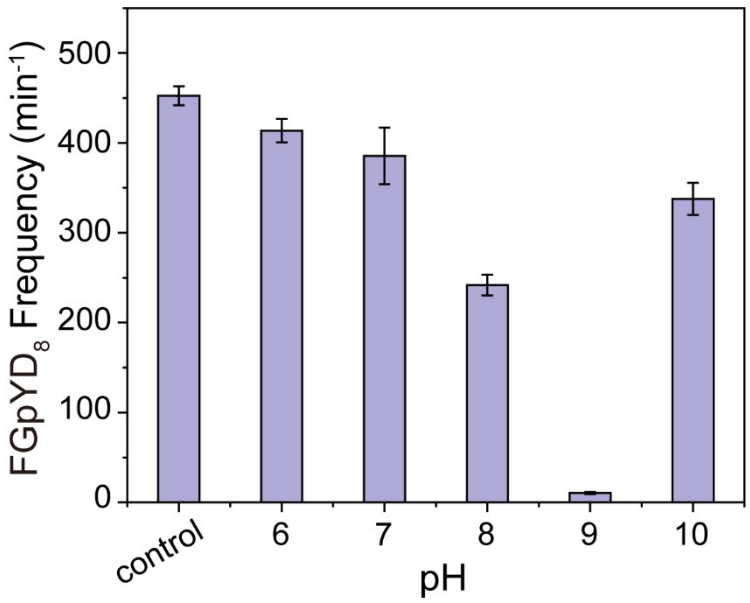

Supplementary Figure 6. Effect of pH on the alkaline phosphatase digestion. Studies have shown that alkaline phosphatase exhibits its highest activity under slightly alkaline conditions (pH 8.0-10.0)[4]. Given that the peptide probe used as alkaline phosphatase in this work contains a large number of negative charges, which may affect its interaction with the enzyme, we optimized the pH conditions of the enzymatic reaction to ensure a highly efficient response of the probe to the enzyme: we performed an enzyme immunoassay using 100.0 ng/mL $VEGF_{165}$ and 50.0 μM $FGpYD_8$. After the reaction, 2.0 μL of the product was mixed with 5.0 μL of CB[7] (5.0 mM) and tested. The frequency of $FGpYD_8$'s characteristic signals was counted (Figure 2c). The condition with the lowest event frequency indicated the most efficient probe cleavage; this was observed at pH 9.0, which was therefore used for further experiments. All data were acquired in the buffer of 3.6 M KCl, 10.0 mM PBS, pH 5.0 in trans, 1.0 M KCl, 10.0 mM PBS, pH 5.0 in cis, with the transmembrane potential held at +200 mV. Number of individual experiments n = 3.

Supplementary Table 1.

Name	DNA Sequence (5'-3')	Modification
DNA 1	ACCCTTGTACCAGTGTTCGAAGATCCACTGG TACAAGGGTTGGGAGATTTTTTTTT	3'-Biotin
DNA 2	CCCTTGTACCAGTGTTCGAAGATCTCACTGG TACAAGGGTTGGGAGATTTTTTTT	3'-Biotin
DNA 3	CCTTGTACCAGTGTTCGAAGATCTGCACTGG TACAAGGGTTGGGAGATTTTTTTTT	3'-Biotin
DNA 4	ACTGGTACAAGGGTTTTTTTTTT	3'-Biotin
DNA 5	CACTGGTACAAGGGTTTTTTTTTT	3'-Biotin
DNA 6	ACACTGGTACAAGGTTTTTTTTTT	3'-Biotin

Supplementary Table 2.

Name	microRNA Sequence (5'-3')
miR-150-5p	UCUCCCAACCCUUGUACCAGUG
miR-205-5p	UCCUUCAUUCCACCGGAGUCUG
miR-155-5p	UUAAUGCUAAUCGUGAUAGGGGUU
miR-21-5p	UAGCUUAUCAGACUG AUGUUGA
let-7a-5p	UGAGGUAGUAGGUUGUAUAGUU

References:

1. M. Wanunu, W. Morrison, Y. Rabin, A. Y. Grosberg and A. Meller, Nat. Nanotechnol., 2010, 5, 160-165.
2. K. J. Freedman, L. M. Otto, A. P. Ivanov, A. Barik, S. H. Oh and J. B. Edel, Nat. Commun., 2016, 7, 10217.
3. X. Chen, Y. Zhang, G. Mohammadi Roozbahani and X. Guan, ACS Appl. Bio Mater., 2019, 2, 504-509.
4. M. H. Ross, J. O. Ely and J. G. Archer, J. Biol. Chem., 1951, 192, 561-568.